JOURNAL OF CATALYSIS **171,** 467–475 (1997)
ARTICLE NO. CA971796

Effect of Phase Composition of the Oxidic Precursor on the HDS Activity of the Sulfided Molybdates of Fe(II), Co(II), and Ni(II)

Joaquín L. Brito[1] and A. Liliana Barbosa[2]

Laboratorio de Fisicoquímica de Superficies, Centro de Química, Instituto Venezolano de Investigaciones Científicas, IVIC, Apartado 21827, Caracas 1020-A, Venezuela

Received March 5, 1997; revised June 16, 1997; accepted June 17, 1997

The catalytic HDS activities of unsupported sulfided molybdates of Fe(II), Co(II), and Ni(II) have been examined measuring the conversion of thiophene at 400°C under atmospheric pressure. The oxidic precursors employed included the hydrates $A\mathrm{MoO_4}\cdot\mathrm{H_2O}$ and the α- and β-$A\mathrm{MoO_4}$ polymorphs (A = Fe, Co, or Ni). The previous finding that sulfided β-$\mathrm{NiMoO_4}$ is a better HDS catalyst than α-$\mathrm{NiMoO_4}$ is now generalized to the other two molybdate systems, suggesting that the tetrahedral environment of Mo in the β-isomorphs provides a more active A–Mo–S phase than the octahedral one in the α-molybdates. The reduced (nonpresulfided) molybdate samples showed lower HDS activities than those sulfided in pure $\mathrm{H_2S}$. Prereduction followed by sulfiding seems to be an optimum procedure for the highest HDS activity of the nickel molybdates and also of β-$\mathrm{FeMoO_4}$. It was found that $\mathrm{NiMoO_4}\cdot\mathrm{H_2O}$ renders a more active sulfided catalyst than the β-phase synthesized by calcination at 760°C, and this seems to be related to the *in situ* generation of β-$\mathrm{NiMoO_4}$ with higher surface area during the activation of the hydrate at 400°C. The hydrated phase of cobalt behaved similarly, but that of iron, on the contrary, was a poorer catalytic precursor than β-$\mathrm{FeMoO_4}$. It is suggested that decomposition of the hydrated compound in the case of Fe could generate a more crystalline material upon sulfiding due to the possibility of changes in the oxidation state of the metals (i.e., $\mathrm{Fe^{2+}} \rightleftarrows \mathrm{Fe^{3+}}$, $\mathrm{Mo^{6+}} \rightleftarrows \mathrm{Mo^{5+}}$) during thermal transformations in presence of evolved water.

INTRODUCTION

Research in the field of hydrodesulfurization (HDS) catalysis has been carried out during the past 50 years. Catalyst formulations consisting of "cobalt molybdate" on alumina were first empirically developed and optimized by *trial and error* approaches. Later, nickel–molybdenum formulations were found to be active and also empirically optimized. This type of work was pursued almost exclusively in the industrial laboratories (1). After about 1965, groups in academic institutions became increasingly involved in research on these catalytic systems, focusing their attention in the oxidic precursors of the catalysts, as it was shown early that the active (sulfided) state is very sensitive to exposure to ambient conditions and consequently difficult to handle without special *in situ* techniques. With the development of such techniques, it became feasible to study the active sulfides, with the result that now most emphasis in research on the catalytic systems is put on the sulfided state. However, catalysts in the oxidic state are important materials themselves, as is evident considering that the catalysts are fully oxidized not only when originally prepared, but also after regeneration procedures that play an important role in the technology of HDS processes (2). In addition, Fe, Co, and Ni molybdates are important components of industrial catalysts for partial oxidation of hydrocarbons (3).

The molybdates of divalent Fe, Co, and Ni of general formula $A\mathrm{MoO_4}$ exist in three distinct phases. Two of them occur under ambient pressure, while the other one ($A\mathrm{MoO_4}$-II) is observed at higher pressures. In the most used nomenclature system, the normal pressure isomorphs are designated α- and β-$A\mathrm{MoO_4}$ (4), where the α prefix accounts for the STP stable phase and β corresponds to the high-temperature modification. In the case of Fe, Co, and Ni, the three α-phases are isotypic, with Mo and the second metal both in octahedral coordination; the β-isomorphs are also isotypic and present Mo in tetrahedral coordination, the group VIII metal being again octahedrally coordinated. While pure β-$\mathrm{NiMoO_4}$ is unstable below about 250°C (5), β-$\mathrm{CoMoO_4}$ and β-$\mathrm{FeMoO_4}$ can be stabilized at room temperature, depending on their thermal history (4, 6). Of relevance for catalytic applications and model studies, this family of compounds can be prepared by soft chemical routes (coprecipitation of $A\mathrm{MoO_4}\cdot n\mathrm{H_2O}$ phases followed by calcination at relatively low temperatures), as opposed to the high-temperature ceramic-type preparations generally employed for structural studies.

[1] To whom correspondence should be addressed at IVIC/BAMCO CCS-199-50, P.O. Box 025322, Miami, FL 33102-5322. Fax: x-58-2-504-1350. E-mail: joabrito@ivic.ivic.ve.

[2] Current address: Universidad de Cartagena, Campus de Zaragocilla. Cartagena, Colombia.

0021-9517/97 $25.00

The industrial HDS catalysts of composition Co(Ni)–Mo/Al_2O_3 typically consist of several surface species (7). Among these, molybdates of the type $AMoO_4$ have been detected several times (see, e.g., 8). Such compounds or mixed-oxide surface species resembling them may have practical importance, as they may help to prevent loss of the Co or Ni promoter into the lattice of the alumina support caused by oxidative treatments, especially during regeneration (2). On the other hand, these mixed phases could be optima precursors for the *A*–Mo–S structures, proposed to be the true active components of the sulfided catalysts (7, 9). However, earlier work had generally reported that molybdates, and particularly $CoMoO_4$, are poor precursors of sulfided HDS catalysts (10). Iron is regarded as a poorer promoter for Mo-based hydrotreatment catalysts than Co or Ni (11), and in consequence it has been employed less frequently, either as a secondary promoter associated to Co and/or Ni (12) or in Fe–Mo formulations (13). An important characteristic of Fe compounds that may explain the low activity of Fe–Mo catalysts is the high probability of forming Fe^{3+} ions in aqueous solutions exposed to atmospheric oxygen (i.e., during impregnation, drying, and calcination of the oxidic precursors of catalysts), even if starting from ferrous salts.

In a previous report (14) we showed that β-$NiMoO_4$ is a better precursor than α-$NiMoO_4$ for unsupported model catalysts employed in the HDS of thiophene. The objective of the present work is to investigate the similar Co and Fe molybdate systems to verify if the higher activity found for the β-phase of Ni is a general fact that might be related to structural considerations. The hydrated $AMoO_4 \cdot nH_2O$ phases obtained as intermediates during the syntheses were also tested.

EXPERIMENTAL

Preparation of Catalysts

The hydrated precursors of general formula $AMoO_4 \cdot nH_2O$ were synthesized by coprecipitation from aqueous solutions of A^{2+} salts and ammonium heptamolybdate. A preparation method was followed which was devised by Mazzocchia *et al*. for $NiMoO_4$ (15). This procedure requires careful control of the temperature and pH of solutions before and after mixing. It was found that temperatures within a short range (80–85°C) and similar pH values (~5 following precipitation of $AMoO_4 \cdot H_2O$) were adequate for the three compounds. It must be emphasized that temperature control must be carried out during coprecipitation, filtration, and washings; otherwise, the molybdates could be decomposed if enough solvent is in contact with the moist precipitate at lower temperatures.

Nickel or cobalt nitrates were employed as precursors salts for the corresponding molybdates and ammonium ferrous sulfate was used for the Fe–Mo system. In the latter case, a special reactor was devised in order to control the atmosphere surrounding the coprecipitation solutions and the solid being filtered, as an inert atmosphere is necessary to guarantee that the iron in the aqueous system remains in the ferrous state. The reactor consisted of a jacketed cylindrical flask, with a porous plate sealed in a side arm. Inert gas (high-purity N_2) was circulated through a tube immersed in the solution. The side arm with porous plate was used both for letting out the inert gas during purging, synthesis, and aging of the precipitate and for filtering the solution without having to remove the solid from the inert atmosphere. Nitrogen was bubbled through all solutions and washing liquids, to displace dissolved oxygen. The temperature of the synthesis vessel was controlled by means of a thermostatic circulator bath connected to the glass jacket of the reactor. After washings, the precipitate was kept into the reactor for an additional 2 h at ~80°C under inert atmosphere before removing and storing in sealed ampoules.

In general, the α-isomorphs of the different compounds were prepared by firing at 550°C the hydrated precursors and cooling slowly to room temperature (~5°C/min). Heat treatments of the iron compounds were always carried out under inert gas atmosphere to prevent the oxidative decomposition of $FeMoO_4$ to $Fe_2(MoO_4)_3$ (16); such effect has not been reported for $CoMoO_4$. In the cases of Co and Fe, thorough grinding of the calcined product was necessary to complete the transformation, as the β-phases can be quenched at room temperature.

The β-isomorphs of Co and Fe were prepared by calcining samples of the α-phase at 550°C, followed by fast cooling (~100°C/min) to room temperature. The standard preparation of β-$NiMoO_4$ consisted in calcination of the α-isomorph at 760°C for 5 min and cooling to the temperature required for further work, always above ~300°C. It has been shown elsewhere (14) that this procedure guarantees the complete transition from α- to β-$NiMoO_4$. As will be discussed below, decomposition of the hydrates at temperatures between 300 and 500°C also result in formation of the β-$AMoO_4$ phases (although with higher surface areas). In general, reference to β-$AMoO_4$ phases should be understood to mean those obtained by calcination of the corresponding α ones at 550 or 760°C.

Note that the surface areas of β-$NiMoO_4$ cannot be measured by standard physisorption techniques. Thus, in order to compare the catalytic properties of α- and β-isomorphs with similar surface areas, some samples of α-$NiMoO_4$ were prepared by cooling the standard β-phase and allowing the $\beta \rightarrow \alpha$ transformation to take place at room temperature. It is assumed that the area of the β-phase is similar to that of the α one obtained by this method. In agreement with this assumption, in the cases of Co and Fe the areas of both phases before and after allowing the transition were comparable.

Catalytic HDS Activity

Thiophene HDS activity at 400°C was measured as reported earlier (14), using a continuous-flow microreactor operating at atmospheric pressure. Samples of catalysts (50 mg) were submitted to one of the pretreatment procedures (see next section) before admitting the reaction feed (120 $cm^3 \cdot min^{-1}$ of H_2 and 1.3×10^{-4} $mol \cdot min^{-1}$ of thiophene). The analysis of reactants and products was carried out with an on-line gas chromatograph and a double-valve system for sampling (17). All samples were measured by duplicate or triplicate. The reproducibility was better than 5%.

Pretreatments

Presulfiding in pure H_2S was accomplished by heating the sample in He to 400°C and admitting a 50 $cm^3 \cdot min^{-1}$ flow of undiluted H_2S. After 1 h, the H_2S flow was discontinued and the reactant mixture was admitted to the reactor. Prereduction was carried out by heating the sample in He to 300°C and then flowing 100 $cm^3 \cdot min^{-1}$ of H_2 for 1 h. Afterward, the temperature was raised to 400°C and thiophene was introduced for reaction measurements.

A second procedure for sulfiding was also employed, which has been previously shown to be the best pretreatment in our reaction conditions for Ni–Mo/Al_2O_3 catalysts (18): After prereduction as above, the temperature was raised to 400°C and H_2S admitted for 1 h. Finally, the H_2S flow was discontinued and the reaction feed was switched on.

Catalyst Characterization

Samples of the hydrated precursors and calcined α- and β-phases were characterized by X-ray diffraction (XRD) with a Philips PW 1730 equipment, employing Fe-filtered Co ($K\alpha$) radiation. BET surface areas were determined by N_2 physisorption in a Micromeritics ASAP 2000 instrument. Fourier transform infrared (FTIR) and photoacoustic (PAS-FTIR) spectra were collected with a Nicolet 5DXC apparatus, using a MTEC 200 attachment for PAS. FTIR samples were analyzed employing the conventional KBr disk technique, while samples for PAS-FTIR were studied as powders. Temperature-programmed reduction (TPR) profiles were obtained by means of a TPD/TPR 2900 instrument from Micromeritics, heating at 20°C/min from ambient to 1000°C (except, as noted above, for β-$NiMoO_4$ where heating was done from ~300°C after *in situ* generation of this phase); sample weight was 10 mg and the reducing gas was 15% H_2 in N_2, flowing at 50 ml/min. Metal chemical analyses were made by means of atomic absorption with a Varian GTA-95 instrument, while sulfur analyses were performed with a Fisons1800 CHNS-O elemental analyzer.

RESULTS

Characterization of the Oxidic Precursor Samples

The coprecipitation method employed for the synthesis of the hydrated molybdates resulted in finely powdered solids. Chemical and thermogravimetric analyses produced the data shown in Table 1, confirming the $AMoO_4 \cdot H_2O$ stoichiometry for the three hydrates. XRD results, showing quite broad signals (Fig. 1), agree with the JCPDS powder diffraction file cards (19) for $NiMoO_4 \cdot H_2O$ (No. 13-128) and $CoMoO_4 \cdot H_2O$ (No. 26-477). No XRD data seem to be available in the literature for the hydrated ferrous molybdate. It was found that increasing contact times of the $FeMoO_4 \cdot H_2O$ compound with the mother liquor during preparation—even under inert atmosphere—led eventually to ferric compounds, in particular, ferrimolybdite (20).

Table 1 also shows some physicochemical characteristics of the anhydrous samples. Good agreement of the measured XRD traces (Fig. 1) with the JCPDS file was observed

TABLE 1

Physicochemical Characteristics of the Oxidic $AMoO_4 \cdot nH_2O$ Catalytic Precursors

Sample	Calcination/drying temperature (°C)	Color	Composition atomic ratio ($A/(A+Mo)$)	BET surface area ($m^2 \cdot g^{-1}$)	TGA weight loss at 150°C (mol ratio $H_2O/AMoO_4$)
$NiMoO_4 \cdot H_2O$	110	Golden yellow	0.49	37	0.9
α-$NiMoO_4$	550	Yellow	0.51	38	—
β-$NiMoO_4$	760	Greenish-yellow	0.53	26	—
$CoMoO_4 \cdot H_2O$	110	Violet	0.48	18	0.9
α-$CoMoO_4$	550[a]	Green	0.49	24	—
β-$CoMoO_4$	550	Violet	0.48	20	—
$FeMoO_4 \cdot H_2O$	110[b]	Light brown	0.47	8	1.0
α-$FeMoO_4$	550[a,b]	Dark brown	0.45	9	—
β-$FeMoO_4$	550[b]	Brown	0.47	7	—

[a] Ground to complete $\beta > \alpha$ transition.
[b] Dried/calcined under inert gas.

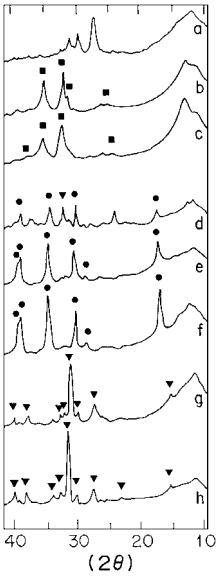

FIG. 1. Powder XRD patterns of (a) $FeMoO_4 \cdot H_2O$; (b) $CoMoO_4 \cdot H_2O$; (c) $NiMoO_4 \cdot H_2O$; (d) α-$FeMoO_4$; (e) α-$CoMoO_4$; (f) α-$NiMoO_4$; (g) β-$FeMoO_4$; (h) β-$CoMoO_4$. Filled squares, $AMoO_4 \cdot nH_2O$ phases; filled circles, α-$AMoO_4$; filled triangles, β-$AMoO_4$.

for α-$NiMoO_4$ (No. 33-948), α-$CoMoO_4$ (No. 25-1434), and β-$CoMoO_4$ (No. 21-868). β-$NiMoO_4$ cannot be quenched—if pure—at room temperature (5, 14), and thus the evidence for the presence of this phase stems mainly from the TPR experiments. However, the $\alpha \rightarrow \beta$ transition in the present samples of $NiMoO_4$ has been confirmed to be completed under the conditions described above (calcination for 5 min at 760°C) in a high-temperature XRD study now in progress (21). The α-isomorphs of $CoMoO_4$ and $NiMoO_4$ were also positively identified by comparing their transmission FTIR spectra (Fig. 2) with published data (22, 23). In the case of β-$CoMoO_4$ (also for β-$FeMoO_4$) the IR spectra were acquired from the powdered samples by means of the PAS attachment, as pressing to form self-supporting waffers or KBr pellets resulted in partial transformation to the α-phases. Although these spectra were poorer than those acquired by FTIR, the comparison with previously reported data for $MgMoO_4$ (22, 23) and $MnMoO_4$ (22) confirmed the presence of the β-isomorphs of the Fe and Co compounds. Note that Mg and Mn molybdates exist in a single normal pressure phase, with Mo tetrahedrally coordinated, which is isomorphous to the β-phase of the iron group molybdates (4).

Most XRD peaks observed for α- and β-$FeMoO_4$ (Fig. 1) agree with the JCPDS data (card Nos. 22-1115 and 22-628, respectively). For β-$FeMoO_4$ the number of peaks and their intensities were in good agreement with the card, but in the case of the α-phase peak intensities do not fully correspond with the data on the card; particularly, some peaks of the β-isomorph are still present, but also other signals are observed which could be due to ferric compounds. The comparison of the (PAS-)FTIR spectra of these samples with those of the Ni and Co compounds confirmed the presence of the α- and β-phases (Fig. 2) but, again, the signals of α-$FeMoO_4$ are rather broad, suggesting that the transition from β- to α-phase has not been completed or that other phases could be present (as β-$FeMoO_4$, ferric molybdate presents Mo ions in tetrahedral coordination).

TPR profiles of the oxidic samples can be seen in Fig. 3, where the characteristic T_m (temperature at the maximum) of each signal is displayed. Quantitative data calculated from these spectra are shown in Table 2. The three molybdate systems show peculiarities that allow to easily distinguish among them by simply examining the shape of the reductograms. TPR spectra of nickel and cobalt molybdates present two peaks, but the ratio of intensities of lower to higher T_m peaks changes from about 4:1 in Ni to 1:4 in Co (Table 2). On the other hand, ferrous molybdates are characterized by a broad, structured, high-temperature signal.

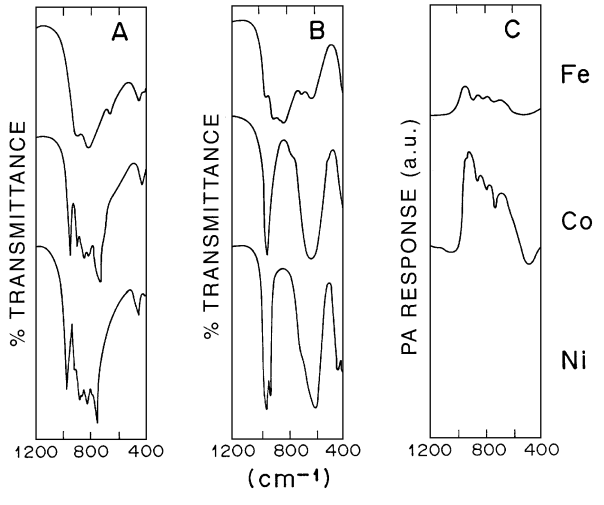

FIG. 2. FTIR (A, B) and PAS-FTIR (C) spectra of (A) hydrated phases; (B) α-phases; (C) β-phases. Top, $FeMoO_4 \cdot nH_2O$; middle, $CoMoO_4 \cdot nH_2O$; bottom, $NiMoO_4 \cdot nH_2O$.

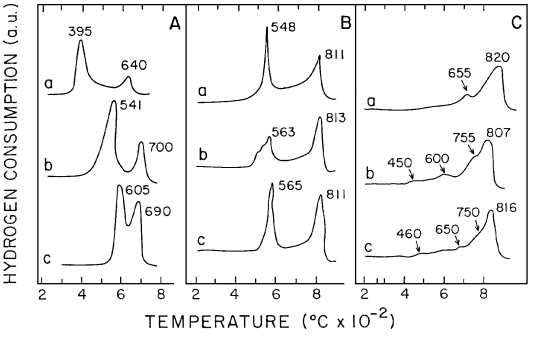

FIG. 3. TPR profiles of (A) $NiMoO_4 \cdot nH_2O$; (B) $CoMoO_4 \cdot nH_2O$; (C) $FeMoO_4 \cdot nH_2O$; (a) hydrated phases; (b) α-phases; (c) β-phases.

TABLE 2

Quantitative TPR Data

Sample	H_2 consumption/mmol · gcat^{-1}	
	Total	First peak
$NiMoO_4 \cdot H_2O$	16.2	13.5
α-$NiMoO_4$	18.5	15
α-$NiMoO_4$[a]	18.3	14.9
β-$NiMoO_4$	18.2	13.4
$CoMoO_4 \cdot H_2O$	16.5	4.1
α-$CoMoO_4$	18.3	4.7
β-$CoMoO_4$	17.8	4.1
$FeMoO_4 \cdot H_2O$	18.1	—
α-$FeMoO_4$	19.8	—
β-$FeMoO_4$	17.6	—

[a] Calcined at 760°C for 5 min.

Similar profiles of the hydrated (24) and anhydrous (14, 24) $NiMoO_4$ phases have been previously reported and discussed. The different TPR spectra of α- and β-$NiMoO_4$ (Fig. 3A) allow us to confirm the presence of the latter phase in the corresponding sample (14). Mazzocchia and Di Renzo also found that the α- and β-phases of $NiMoO_4$ show different rates of reduction (25). The quantitative results (Table 2) agree with a reduction mechanism in two steps, the first one (major peak at lower temperature) related to the formation of Ni, Mo, and Ni–Mo alloys or intermetallics, dispersed in a small amount of amorphous MoO_2, which becomes reduced under the high T_m signal (24). Reduction of the anhydrous nickel molybdates seems to occur through decomposition to NiO plus MoO_2, and no mixed lower oxides have been detected (25), contrary to the cobalt and iron molybdates (see below).

Cobalt molybdate reduction was studied by Haber and Janas (26). These authors found, under isothermal conditions (480 to 540°C), reduction of either anhydrous phase to an equimolar mixture of $Co_2Mo_3O_8$ (molybdite) and Co_2MoO_4 (spinel). The present TPR data agree, showing reduction to these lower oxides in a first stage (peak at ~565°C; H_2 consumption shown in Table 2), followed by reduction to the metals at higher temperatures. Only minor differences (in the shape of the low-temperature peak) exist between the TPR profiles of α- and β-phases of $CoMoO_4$, which probably is due to the fact that the $\alpha \rightarrow \beta$ transition temperature at 420°C (27) is below the onset of the reduction under TPR conditions (Fig. 3). Both Ni- and Co-hydrated molybdates are easier to reduce than their anhydrous counterparts, but in general they show similar features to those of the later. Other studies of $CoMoO_4$ reduction have confirmed the findings of Haber and Janas (see 28 and references therein).

For iron (II) molybdate reduction less data are available in the literature. Pasquon *et al*. (29) reported that *isothermal* hydrogen reduction of β-$FeMoO_4$ at 500°C (several hours) produces $FeMoO_3$. However, in the transient conditions of the present TPR experiments, reduction starts at higher temperature (close to 700°C), with complete reduction to the metals in a single or two closely overlapping peaks. In a study of catalysts composed of mixtures of $Fe_2(MoO_4)_3$ and MoO_3 by means of TPR, XRD, and Mössbauer spectroscopy, Zhang *et al*. showed that β-$FeMoO_4$—obtained *in situ* by reduction of $Fe_2(MoO_4)_3$—is reduced to $Fe_2Mo_3O_8$ and Fe_3O_4 at 680°C and to the metals at 730°C (30). These somewhat lower temperatures, compared to those in the present study, are probably due to the use of different experimental setup and conditions (10°C · min^{-1} heating rate, 20 mg sample, etc.); also, the reduction of a considerable amount of a Fe^{3+} phase could help in activating H_2 at lower temperatures. The small signals between 400 and 650°C observed in the present samples could be related to the presence of low amounts of other Fe and Mo compounds as impurities, in agreement with the XRD data. Note that the amounts of H_2 consumed in the reduction of both the hydrate and the α-isomorph are significantly higher than that of β-$FeMoO_4$ (Table 2), suggesting a higher content of Fe^{3+} impurities in the first two cases. Otherwise, the present results show little, if any, differences between α- and β-$FeMoO_4$, which could be the result, as in the case of $CoMoO_4$, of the reduction temperatures being higher than those of the $\alpha \rightarrow \beta$ transition.

Catalytic HDS Activity

Catalytic activity for the HDS of thiophene is reported as pseudo-first-order rate constants for thiophene disappearance (Fig. 4). Activity vs time plots were similar to those shown elsewhere for the anhydrous Ni molybdates (14), characterized by higher initial activities which decreased to steady state values within the first 40 min. Figure 4a shows the steady-state catalytic activities of samples presulfided in pure H_2S. As reported previously (14), sulfided β-$NiMoO_4$ showed higher HDS activity than the sulfided α-isomorph. Analogous results were found for the α- and β-phases of $CoMoO_4$ and $FeMoO_4$ submitted to both presulfiding treatments (Figs. 4a and 4c), but after prereduction differences between the activities of either anhydrous phase were almost negligible (Fig. 4b). Interestingly, the activities of $NiMoO_4 \cdot H_2O$ and $CoMoO_4 \cdot H_2O$ were higher than those of the corresponding anhydrous phases regardless of the pretreatment employed (Fig. 4). This is not the case for the ferrous molybdates; only for the reducing pretreatment (Fig. 4b) the activity of the hydrated phase was higher than those of the anhydrous polymorphs.

In general, the activities of Ni-containing catalysts were higher than those of the Co or Fe systems. This result is consistent with previous reports, e.g., those of Takhur *et al*. (31). Surprisingly, the HDS activity of β-$FeMoO_4$ is similar to that of β-$CoMoO_4$. Although Fe–Mo catalysts have been shown to render higher HDS activity than those

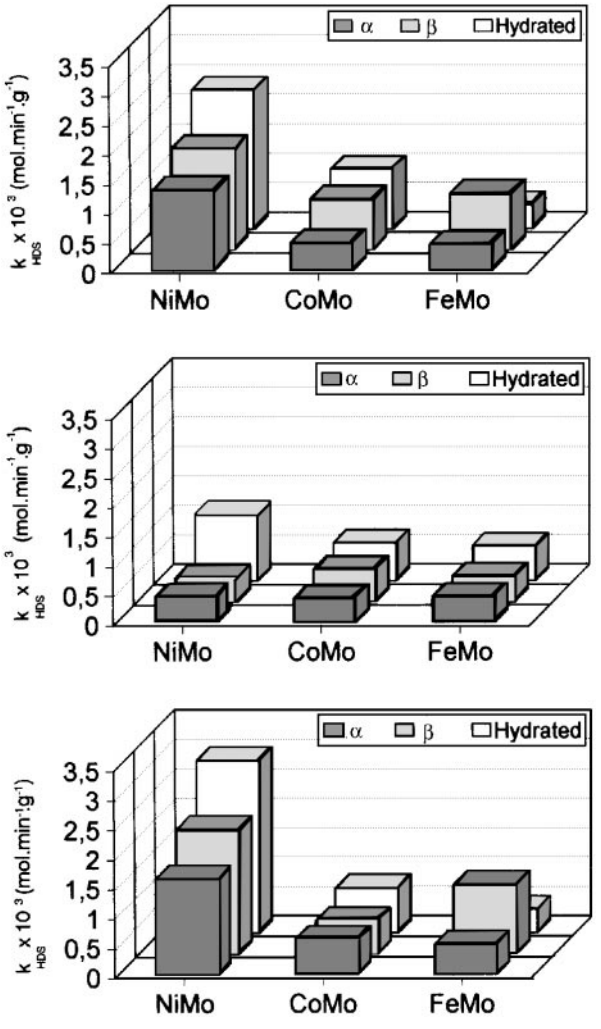

FIG. 4. Effect of composition and pretreatment on steady state thiophene HDS activity of sulfided $A MoO_4 \cdot nH_2O$ phases. Pretreatments: top, H_2S, 1 h, 400°C; middle, H_2, 1 h, 300°C; bottom, H_2, 1 h, 300°C + H_2S, 1 h, 400°C.

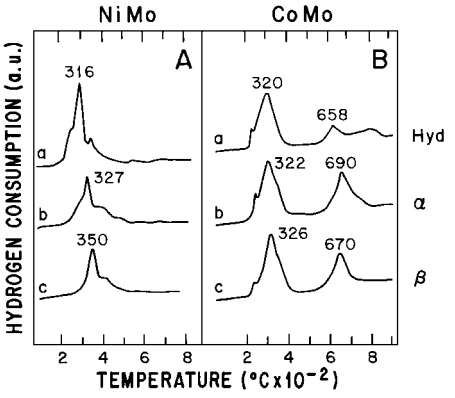

FIG. 5. TPR profiles of samples sulfided 1 h at 400°C in pure H_2S. (A) $NiMoO_4 \cdot nH_2O$; (B) $CoMoO_4 \cdot nH_2O$; (a) hydrated phases; (b) α-phases; (c) β-phases.

with only Mo, they are generally reported to be less active than Co–Mo and Ni–Mo catalysts (31). Most cases where these synergistic effects are found for Fe–Mo involve direct preparation of the active sulfides, e.g., by coprecipitation from salts of Fe and Mo in the presence of sulfur compounds (e.g., 31).

Characterization of Sulfided Samples

Several sulfided samples were submitted to TPR and XRD measurements and analyzed for sulfur contents. The TPR patterns of NiMo samples sulfided in pure H_2S at 400°C (Fig. 5A) present a structured signal centered between 315 and 350°C, corresponding to labile sulfur (S_x) (32); H_2 consumption is completed at about 550°C, and no additional TPR peaks are seen up to 900°C. Table 3 shows that sulfur contents in freshly sulfided samples are slightly above the "$NiMoS_4$" stoichiometry (calculated S content for "$NiMoS_4$," 45.34 wt%), while samples treated with H_2 at 400°C for 1 h after sulfiding tend to the composition corresponding to the thermodynamically stable compounds (in HDS reaction conditions) $Ni_3S_2 + MoS_2$ (35.62 wt% theoretical S content). These results confirm our previous estimations based on quantitative TPR (14). Gachet *et al.* (33) also reported S/(Mo + Ni) ratios up to 2.1 for freshly prepared, unsupported Ni–Mo sulfided catalysts. After HDS reactions, those ratios decreased to the value corresponding to the mixture of $Ni_3S_2 + MoS_2$. XRD patterns of the present NiMo samples were similar to those reported elsewhere (14), suggesting very amorphous sulfide structures.

The CoMo compounds present TPR patterns consisting of two broad signals (Fig. 5B). The low-temperature peaks, between 320 and 326°C, agree with those found for sulfided NiMo (Fig. 5A) and also for silica-supported, Ni–Co–Mo-sulfided samples (34) and are assigned to S_x, labile sulfur. On the other hand, the high-temperature peaks (at 660–690°C) are at temperatures too high to be assigned to S_x.

TABLE 3

Sulfur Contents of NiMo and CoMo Samples

Sample	Sulfur content/wt%	
	Freshly sulfided[a]	Postreduced[b]
$NiMoO_4 \cdot H_2O$	46.8	35.9
α-$NiMoO_4$	46.3	36.8
β-$NiMoO_4$	45.9	37.3
$CoMoO_4 \cdot H_2O$	43.1	35.8
α-$CoMoO_4$	44.8	36.2
β-$CoMoO_4$	42.6	34.1

[a] Sulfided in pure H_2S at 400°C for 1 h.

[b] Sulfided in pure H_2S at 400°C for 1 h and reduced in H_2 at 400°C for 1 h.

Both *bulk* Co_9S_8 (32) and amorphous MoO_2 of small particle size (35) show TPR peaks in the same temperature region. XRD patterns of the sulfided CoMo samples (not shown) present small peaks at $2\theta = 26.1$ and 37.2° ($d = 3.41$ and 2.42), characteristic of MoO_2 (JCPDS card No. 5-452), while no peaks of sulfide species distinct from MoS_2 are seen. In consequence, the TPR peaks at 660–690°C are assigned, at least in part, to MoO_2 highly dispersed in the sulfide matrix. This MoO_2 component can account for the low sulfur contents compared to the calculated stoichiometries for "$CoMoS_4$" (45.30 wt% S, compare with freshly sulfided samples in Table 3) or $Co_9S_8 + MoS_2$ (37.43 wt% S, compare with sulfided samples postreduced at 400°C).

DISCUSSION

Oxidic and Reduced Catalytic Precursors

The characterization study of the oxidic precursors confirms that the Ni and Co molybdate samples are the very pure monohydrates and the α- and β-isomorphs. Iron seems to be a more complex system, and the phase purity of the α-$FeMoO_4$ sample is not as good as for the Co and Ni molybdates or the β-$FeMoO_4$ isomorph. However, chemical analysis suggests that the impurities are other Fe and/or Mo compounds, most probably in oxidic form. The hydrated ferrous molybdate was particularly sensitive to preparational parameters. For example, prolonged aging (several hours) in the synthesis reactor in contact with the mother liquor, even under inert atmosphere, eventually resulted in formation of ferrimolybdite, $Fe_2(MoO_4)_3 \cdot nH_2O$, as shown by the characteristic XRD trace (20). It could be assumed that the impurities of the ferrous molybdate samples are simple or mixed oxides of Fe and Mo, with a strong possibility of $Fe_2(MoO_4)_3$ being present. In this regard, Védrine *et al.* (6) reported that mixed Co–Fe^{2+} molybdates always contain a proportion of Fe^{3+} ions, regardless of precautions taken in the synthesis, and that ferric ions seem to stabilize the α-phase.

The reducibilities vary strongly with the group VIII metal. The TPR data indicate that the Ni molybdates are reduced to the metallic state at $\leq$600°C, while the Co and Fe compounds only reduce to the metal at about 800°C. Temperatures as low as 250°C have been reported under isothermal conditions for the reduction of hydrated $NiMoO_4$ to the metallic state (36), while the anhydrous phases can be reduced isothermally at 370°C (25); Tsurov *et al.* (37) noted that reduction to the metals is thermodynamically possible above about 350°C. On the other hand, the cobalt molybdates show the formation of mixed lower oxides by reduction at temperatures typically employed for pretreatment and operation of HDS catalysts, e.g., at 400°C (38). The iron molybdates are almost unreducible at similar temperatures in the transient conditions of the TPR experiments, as shown in this work and also by Zhang *et al.* (30), but long-time reduction at about 500°C proceeds to Fe–Mo oxides with Mo oxidation state lower than +6 (29). In both the Co and the Fe cases reduction to the metals is hindered by the formation of stable intermediate oxides (molybdite and spinel phases), which are not observed in the $NiMoO_4$ system (25). Most probably, the different reducibilities of the oxidic precursors should have an effect regarding the generation of the active species and their activity. In connection with the present results, it must be noted that the stronger effect of the Ni promoter (compared to Co) on the reducibility of Mo in alumina-supported catalysts has been noted previously (39), which establishes a clear difference in the supported catalysts as well as in the unsupported molybdate phases between Ni and Co as promoters.

It is important to lay stress on the fact that calcination of the hydrated phases produces the β-isomorphs at rather low temperatures. This fact, known for the Co (27) and Fe (4) systems, was only recently reported for $NiMoO_4 \cdot H_2O$ (40); similar data have also been found using the present $NiMoO_4 \cdot H_2O$ sample in a high-temperature XRD study (21). In the case of Fe, drying and calcination must be performed in the absence of air. Even if this is accomplished, structural rearrangements during heat treatments could be facilitated by the possibility of local redox cycles (e.g., $Fe^{2+} \rightleftarrows Fe^{3+}$; $Mo^{6+} \rightleftarrows Mo^{5+}$) in the presence of autogenous water. A consequence of such processes would be the low surface areas of the ferrous molybdates compared to the other two systems.

Catalytic Activity

The HDS activity of mixed Ni–Mo sulfides is higher than those of the Co–Mo and Fe–Mo ones, in agreement with previous reports (31). The higher reducibility of the Ni–Mo oxides may be connected to this fact, ensuring that the Ni molybdates are easier to sulfide than either of the other two molybdate systems. Note particularly that preredution followed by sulfiding of Ni–molybdates render higher HDS activities than plain presulfiding with pure H_2S, which is not the case for the Co and Fe systems (Fig. 4). The difference between those compounds that could explain the diverging activity behavior in this case is that Co– (and Fe–) molybdate, under the preredution conditions employed in this work, tend to produce lower oxides (molybdite and spinel, main molybdenum species: Mo^{4+}) which should be more difficult to sulfide than the original compound (41). On the other hand, $NiMoO_4$ is potentially reducible to the metals plus a minor amount of MoO_2. Although the latter could be, in principle, difficult to sulfide (except if it is very porous) (35) the metals should be easily converted to the sulfides (42).

In previous literature (10) $CoMoO_4$ was described as a poor precursor compound for sulfides to be employed as HDS catalysts. More recently, from thiophene HDS

experiments carried out by means of a pulse technique, Korányi *et al*. (43) also stated that the behavior during activation of unsupported catalysts containing mainly $CoMoO_4$ was different from (much less active than) supported $Co–Mo/Al_2O_3$ and thus they neglected that this compound could be the precursor of active sulfided species. It should be noted that in both these studies the $CoMoO_4$ precursors were prereduced (but not sulfided) before reaction. The present results suggest that active sulfided phases can be obtained (with a proper sulfiding treatment) from $CoMoO_4$, especially from the β-isomorph, by preventing extensive reduction prior to sulfidation.

Contrary to cobalt and nickel, iron is regarded as a poor promoter of Mo-based hydrotreatment catalysts (11, 12). Adachi *et al*. (44) have recently concluded that this is due to the fact that, in the aqueous solutions employed during the preparation of Fe–Mo-supported catalysts, iron exists as ferric ions: As the chemistry of Fe(III) is considerably more complex than that of Fe(II), Co(II) or Ni(II), this would result in differences between the Fe-promoted catalysts and the Co- or Ni-promoted ones that appear even in the oxidic state (44). Our results show that the activity of Fe–Mo catalysts can be comparable to that of Co–Mo, provided that iron is kept in the ferrous state during preparation and pretreatments.

As previously found for $NiMoO_4$, the sulfided β-isomorphs of $CoMoO_4$ and $FeMoO_4$ are more active than the corresponding α ones (even after allowing for the presence of a significant amount of β-$FeMoO_4$ in our "α-$FeMoO_4$" sample). This suggests that for the group VIII metal molybdates, the tetrahedral coordination of Mo in the precursor mixed oxides is beneficial to the HDS function of the sulfides. Several workers have reported similar results for Ni-promoted catalysts: Pratt *et al*. (45) found an optimum HDS activity in mixed unsupported Ni–Mo catalysts in the composition range $0.55 \leq Ni/(Ni + Mo) \leq 0.75$; this is the composition range where a stable β-$NiMoO_4$/NiO solid solution exists in the precursor oxide (46). Teixeira da Silva *et al*. (47) suggested that a bidimensional β-$NiMoO_4$ structure supported on alumina can be an optimum precursor for NiMoS active phases. Damyanova *et al*. (48) reported that HDS activity in $Ni–Mo/TiO_2–Al_2O_3$ catalysts correlates with spectroscopic results showing the presence of Mo [Th] species in the catalyst precursor.

Laine and Pratt (49) showed previously that $NiMoO_4 \cdot H_2O$ produces a more active sulfided HDS catalyst than α-$NiMoO_4$. This fact is confirmed in the present work and extended to the $CoMoO_4$ system; also, it is noted that the $NiMoO_4$ and $CoMoO_4$ hydrates render higher activities than either anhydrous (α or β) phase. On the other hand, decomposition of the hydrated compound in the case of Fe might generate a more crystalline material upon sulfiding due to the possibility of changes in the oxidation state of both metals (i.e., $Fe^{2+} \rightleftarrows Fe^{3+}$, $Mo^{6+} \rightleftarrows Mo^{5+}$) during thermal transformations in the presence of evolved water. Such half-cell reactions show a favorable electrode potential in the presence of water for Mo reduction and Fe oxidation (30). Thus, the hydrated Fe–Mo catalyst presents lower activity than anhydrous β-$FeMoO_4$ regardless of the sulfiding procedure, while the corresponding hydrates of Ni and Co are better as precursors than the anhydrous phases.

The formation of a β-$AMoO_4$ phase from Ni- and Co-hydrated molybdates at low temperatures during the pretreatment could be the main reason for the enhanced activity observed for those precursor phases. In the case of Ni, the α-sample produced at 550°C showed higher surface areas than that resulting from the standard calcination at 760°C (Table 1). It may be inferred that dehydration at a lower temperature (400°C) would produce a still higher surface area. On the other hand, if the tetrahedral environment of Mo is important in producing more active catalysts, it should be noted that the coordination of Mo in the hydrates is likely to be tetrahedral, as in the β-phases. Grimblot *et al*. (50) showed by Raman spectroscopy that coprecipitated Ni–Mo dried (uncalcined) samples show signals characteristic of Mo [Th]. The present FTIR spectra of the hydrates are consistent with that observation, as the four characteristic Mo–O signals observed in the β-isomorphs between 600 and 1000 cm^{-1} are also present in the hydrates; on the other hand, the band at 620 cm^{-1}, characteristic of Mo in octahedral environment (Fig. 2B), is absent in both hydrated and β-phases (Figs. 2A and 2C, respectively). Finally, DTA measurements showed no thermal effects during the dehydration of $NiMoO_4 \cdot H_2O$ to the β-phase, while they are clearly observed upon α–β interconversion (51), which suggests that there is not a change in the coordination of Mo in the transition from the hydrates to the β-phases.

The reasons for the higher activity of sulfides derived from the β-phases are uncertain at this time. It has been shown that sulfiding of bulk Mo oxides and of supported, promoted, or unpromoted Mo-based catalysts proceeds by exchange of S for O rather than by reduction and nucleation of a new sulfide phase (42). This suggests that the original structure of the oxidic precursor may have a strong influence on that of the active sulfide phase; this is also in line with observations indicating that the oxidic precursor and active sulfided structures may be reversibly reproduced during activation–regeneration cycles in supported catalysts (2, 47, 52). In general, Mo [Th] species in Mo/Al_2O_3 catalysts are difficult to sulfide (42) or reduce (53). In consequence, most workers have assigned the HDS activity to Mo [Oh] sites in the precursor oxides. However, the rather unreactive Mo [Th] sites in unpromoted alumina-supported catalysts are known to be due to $Al_2(MoO_4)_3$-like surface compounds (53). It is conceivable that supported Mo ions in tetrahedral coordination, associated to the promoters in a stabilized β-molybdate-like phase, could be efficient precursors for HDS active sites.

CONCLUSIONS

From the results discussed above, the following conclusions can be drawn:

(i) Ni–Mo oxidic precursors produce more active HDS sulfided catalysts than the Co–Mo and Fe–Mo compounds, probably because the former can be potentially reduced to the metallic state at lower temperatures, instead of being reduced to lower mixed oxides—more difficult to sulfide—as in the other two cases.

(ii) The higher activities of sulfides derived from the β-phases, compared with the α ones, seems to be a general characteristic of the three group VIII molybdates. It should be related to the coordination of Mo in the oxidic precursors, which is the main difference between both polymorphs.

(iii) The hydrated molybdates of Ni and Co are very good precursors for HDS-sulfided catalysts, probably because they render active phases with better textural properties (higher surface area and/or lower crystallinity). The hydrated ferrous molybdate is not a good precursor for HDS catalysts, which may be due to the possibility of local red-ox processes during activation which can lead to sintering of the sulfided compounds.

(iv) Iron can be an efficient promoter for HDS catalysts, provided that it is kept in the ferrous state during preparation and activation of the catalysts.

ACKNOWLEDGMENTS

Thanks are due to J. Cáceres, B. Griffe, P. Hernández, M. Labady, and E. Marcano for their technical assistance. Support of CONICIT through Programa Nuevas Tecnologías (Grant QF-10), for part of the instrumentation is gratefully acknowledged. A.L.B. thanks Fundación Gran Mariscal de Ayacucho for financial support.

REFERENCES

1. McKinley, J. B., *in* "Catalysis" (P. H. Emmett, Ed.), Vol. V, p. 405. Reinhold, New York, 1957.
2. Madeley, R. A., and Wanke, S., *Appl. Catal.* **39**, 295 (1988).
3. Zou, J., and Schrader, G. L., *J. Catal.* **161**, 667 (1996).
4. Sleight, A. W., Chamberlain, B. L., and Weiher, J. F., *Inorg. Chem.* **7**, 1093 (1968).
5. DiRenzo, F., and Mazzocchia, C., *Termochim. Acta* **85**, 139 (1985).
6. Ponceblanc, H., Millet, J. M. M., Coudurier, G., Legendre, O., and Védrine, J. C., *J. Phys. Chem.* **96**, 9462 (1992).
7. Topsøe, H., Clausen, B. S., and Massoth, F. E., *in* "Catalysis, Science and Technology" (J. R. Anderson and M. Boudart, Eds.), Vol. 11, p. 1. Springer, Heidelberg, 1996.
8. Brito, J. L., and Laine, J., *Appl. Catal.* **72**, 113 (1991).
9. Wivel, C., Candia, R., Clausen, B. S., and Topsøe, H., *J. Catal.* **68**, 453 (1981).
10. Richardson, J. T., *Ind. Eng. Chem. Fundam.* **3**, 154 (1964).
11. Ternan, M., *J. Catal.* **104**, 256 (1987).
12. Beuther, H., Flinn, R. A., and McKinley, J. B., *Ind. Eng. Chem.* **51**, 1349 (1959).
13. Galarraga, C., and Ramírez de Agudelo, M. M., *J. Catal.* **134**, 98 (1991).
14. Brito, J. L., Barbosa, A. L., Albornoz, A., Severino, F., and Laine, J., *Catal. Lett.* **26**, 329 (1994).
15. Mazzocchia, C., Di Renzo, F., and Céntola, P., *Rev. Port. Quim.* **19**, 61 (1977).
16. Trifiró, F., De Vecchi, V., and Pasquon, I., *J. Catal.* **15**, 8 (1969).
17. Laine, J., *J. High Res. Chrom. Chrom. Commun.* **3**, 10129 (1980).
18. Laine, J., *Chem. Eng. Commun.* **37**, 11 (1985).
19. "JCPDS Powder Diffraction File," Int. Centre for Diffraction Data, Swarthmore, PA, 1989.
20. Horn, E., Kurahashi, M., Huang, D., and Wu, C., *Powder Diff.* **10**, 101 (1995).
21. Rodríguez, J. A., Chaturvedi, S., Hanson, J. C., Albornoz, A., and Brito, J. L., "Abstracts of the 15th Meeting of the North American Catalysis Society," p. 52. Chicago, 1997. *J. Phys. Chem.* [submitted].
22. Matsuura, I., Mizuno, S., and Hashiba, H., *Polyhedron* **5**, 111 (1986).
23. Haber, J., Mielczarska, E., and Turek, W., *Z. Physik. Chem. N.F.* **144**, 69 (1985).
24. Brito, J. L., Laine, J., and Pratt, K. C., *J. Mater. Sci.* **24**, 425 (1989).
25. Mazzocchia, C., and Di Renzo, F., *Calorim. Anal. Therm.* **16**, 311 (1985).
26. Haber, J., and Janas, J., *in* "Reaction Kinetics in Heterogeneous Chemical Systems" (P. Barret, Ed.), p. 737. Elsevier, Amsterdam, 1975.
27. Haber, J., *J. Less-Common Metals* **36**, 277 (1974).
28. Arnoldy, P., Franken, M. C., Scheffer, B., and Moulijn, J. A., *J. Catal.* **96**, 381 (1985).
29. Pasquon, I., Trifiró, F., and Caputo, G., *Chim. Ind.* **55**, 168 (1973).
30. Zhang, H., Shen, J., and Ge, X., *J. Solid State Chem.* **117**, 127 (1995).
31. Takhur, D. S., Grange, P., and Delmon, B., *J. Less-Common Metals* **64**, 201 (1979).
32. Mangnus, P. J., Riezebos, A., van Langeveld, A. D., and Moulijn, J. A., *J. Catal.* **151**, 178 (1995).
33. Gachet, C., Paulus, R., de Mourgues, L., Durand, C., and Toulhoat, H., *Bull. Soc. Chim. Belg.* **93**, 681 (1984).
34. Laine, J., Brito, J. L., and Severino, F., *J. Catal.* **131**, 385 (1991).
35. Arnoldy, P., de Jong, J. C. M., and Moulijn, J. A., *J. Phys. Chem.* **89**, 4517 (1985).
36. Astier, M. P., LaCroix, M. L., and Teichner, S. J., *J. Catal.* **91**, 356 (1985).
37. Tsurov, M. A., Afanasiev, P. V., and Lunin, V. V., *Appl. Catal. A: Gen.* **105**, 205 (1993).
38. Gajardo, P., Grange, P., and Delmon, B., *J. Chem. Soc. Faraday I* **76**, 929 (1980).
39. Brito, J. L., and Laine, J., *J. Catal.* **139**, 540 (1993).
40. Mazzocchia, C., Anouchinsky, R., Kaddouri, A., Sautel, M., and Thomas, G., *J. Therm. Anal.* **40**, 1253 (1993).
41. Schrader, G. L., and Cheng, C. P., *J. Catal.* **85**, 488 (1984).
42. Arnoldy, P., van den Heijkant, J. A. M., de Bok, G. D., and Moulijn, J. A., *J. Catal.* **92**, 35 (1985).
43. Korányi, T. I., Szilágyi, T., Manninger, I., and Paál, Z., *Polyhedron* **5**, 225 (1986).
44. Adachi, M., Contescu, C., and Schwarz, J. A., *J. Catal.* **158**, 411 (1996).
45. Pratt, K. C., Sanders, J. V., and Tamp, N., *J. Catal.* **66**, 82 (1980).
46. Di Renzo, F., Mazzocchia, C., Thomas, G., and Vernay, A. M., *React. Solids* **6**, 145 (1988).
47. Teixeira da Silva, V. L. S., Frety, R., and Schmal, M., *Ind. Eng. Chem. Res.* **33**, 1692 (1994).
48. Damyanova, S., Spojakina, A., and Jiratova, K., *Appl. Catal. A: Gen.* **125**, 257 (1995).
49. Laine, J., and Pratt, K. C., *React. Kinet. Catal. Lett.* **10**, 207 (1979).
50. Grimblot, J., Payen, E., and Bonnelle, J. P., *in* "Proceedings of the Fourth International Conference on the Chemistry and Uses of Molybdenum" (H. F. Barry and P. C. H. Mitchell, Eds.), p. 261. Climax Molybdenum Co., Ann Arbor, MI, 1982.
51. Di Renzo, F., and Mazzocchia, C., *Thermochim. Acta* **85**, 139 (1985).
52. Adachi, M., Contescu, C., and Schwarz, J. A., *J. Catal.* **162**, 66 (1996).
53. Chung, K. S., and Massoth, F. E., *J. Catal.* **64**, 320 (1980).